Networks from Liquid Crystalline Segmented Chain Polymers

Ugo Caruso, Barbara Panunzi, Antonio Roviello, and Augusto Sirigu*

Dipartimento di Chimica, Università "Federico II" di Napoli, via Mezzocannone 4, 80134 Napoli, Italy

Received September 29, 1993; Revised Manuscript Received April 4, 1994®

ABSTRACT: The synthesis and the phase behavior of three liquid crystalline polymer networks and of the linear polymers upon which the networks are based are presented. The linear polymers, that are characterized by the presence of $-OC_6H_4$-*p*-$COOC_6H_3$-*o*-OH-*p*-$CH{=}NC_6H_4$-*p*-*O*- groups connected by flexible molecular segments, exhibit enantiotropic liquid crystalline properties of nematic and/or smectic nature. They have been moderately (≤10%) cross-linked by reaction with $ClOCC_6H_4$-*p*-$O(CH_2)_{12}O$-*p*-C_6H_4COCl in an isotropic *o*-dichlorobenzene dilute solution. The networks form as isotropic gels and undergo anisotropization with enthalpy release on cooling at room temperature. No crystallization takes place. Isotropization, accompanied by a DSC detectable endothermic effect, is restored on heating. The neat networks exhibit also mesogenic properties, but the stability of their liquid crystalline phase is decreased with respect to that of the corresponding linear polymers.

Introduction

The interest in liquid crystalline networks that actually or ideally are derived from segmented chain mesogenic polymers is fairly recent[1–5] notwithstanding an early theoretical attention by de Gennes.[6] Such networks may provide ideally simple objects for investigating the mechanical properties of self-ordering systems and, specifically, the coupling between ordering and mechanical action. Their phase properties in the swollen state have been the subject of theoretical attention by Warner and Wang,[3] who have defined the conditions under which the equilibrium between a nematic gel phase and the pure solvent or the isotropic gel may be possible.

We have reported in previous papers[4,5] the phase behavior of two networks based on nematogenic segmented chain polymers of different structure (1 and 2).

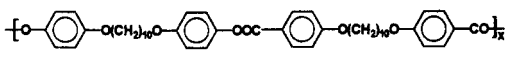

1

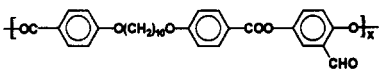

2

In the first case, the network was obtained by reaction of a tricarboxylic acid chloride with an oligomeric variation of the polymer 1 terminally functionalized with 4-hydroxyphenylene groups. In the second case, cross-linking involves the aldehyde group via imine bond formation with a flexible diamine. In both cases the network is formed as an isotropic gel with a low nominal cross-link density. This allowed the permanence in the pure network polymers of the same thermotropic mesomorphism characterizing the parent linear polymers. In both cases the swollen network exhibits optical anisotropy of noncrystalline origin at room temperature and undergoes a thermotropic transition to an isotropic gel phase accompanied by a substantial enthalpy change. The low value of the polymer fraction in the swollen network if compared to the structural flexibility of the network chains and NMR spectroscopy data suggest that, at least for networks based on polymer 2, the anisotropic phase may be solvent-plasticized "solid" polymer better than a single lyotropic phase.

Chart 1

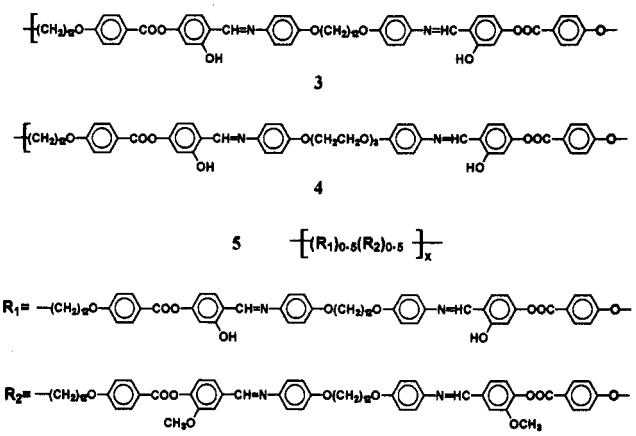

In this investigation, moderately (≤10%) cross-linked networks based on polymers 3–5 (Chart 1) have been prepared and their phase behaviors examined both under swollen and unswollen conditions.

The main scope of our investigation was that of finding new data supporting the view that the behavior underlined is not critically dependent on the specific stereochemical nature of the selected polymer. The results reported confirm this idea. It will be shown that (a) a low cross-link density does not prevent thermotropic liquid crystallinity to show up, (b) cross-linking in an isotropic medium decreases the thermal stability of the mesophase of the neat network as compared to that of the parent linear polymer, and (c) optical anisotropy of noncrystalline origin is exhibited by the swollen network within a definite temperature range. Furthermore, a possible role played by the branch points in reducing the thermal stability of the mesophase in the network will be suggested by use of low molecular weight model compounds.

Experimental Section

Polymer Synthesis. Polymerization was performed in solution following the same basic procedure for all polymers (Scheme 1). A detailed description is reported now for polymer 3. A total of 4.397 g of dialdehyde 6 was dissolved in 40 mL of boiling *o*-dichlorobenzene and 2.477 g of diamine 7 added under a nitrogen atmosphere. A time of 20 min at constant boiling temperature

* Abstract published in *Advance ACS Abstracts*, May 1, 1994.

0024-9297/94/2227-3513$04.50/0

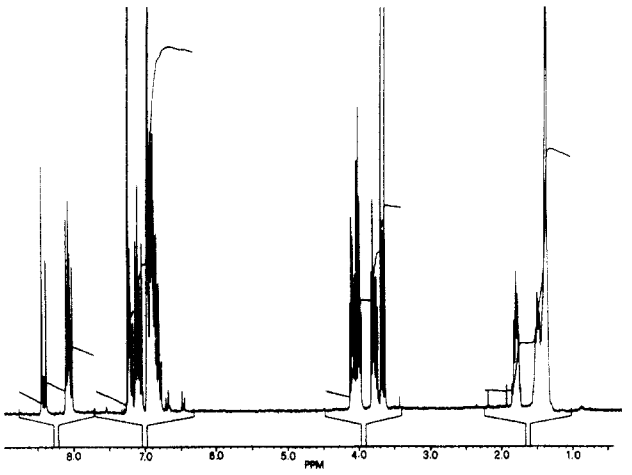

Figure 1. ^{1}H-NMR spectrum of polymer **3** at 130 °C. Solvent: deuterated *o*-dichlorobenzene.

Scheme 1

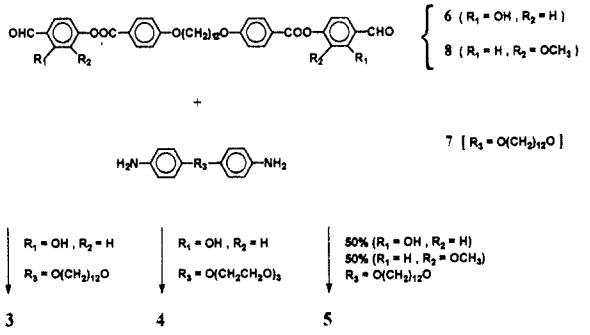

is sufficient to complete the polymerization. The solution is then poured into boiling *n*-hexane and the precipitated polymer washed twice in *n*-hexane and oven-dried at 100 °C. Yields are virtually quantitative. The same procedure has been used for preparing copolymer **5** utilizing equal amounts of the corresponding dialdehydes. The ^{1}H-NMR spectrum in deuterated *o*-dichlorobenzene is coherent with the expected formulas for all polymers. Figure 1 shows the spectrum for polymer **3** as an example.

The key compounds for the polymer synthesis are dialdehydes **6** and **8**. The former was prepared by hydrolysis of imine **9**. E.g.,

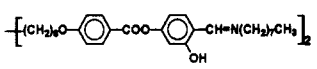

9

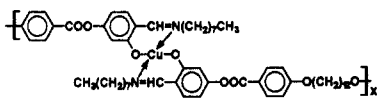

10

20 g of imine **9** are dissolved in 400 mL of dioxane, and ~30 mL of 37% HCl are added. The reaction is let go for ~3 min at ~60 °C. The aldehyde is then precipitated by adding water up to a 1.5-L volume. A further reaction cycle is then performed similarly to the first one but using diluted hydrochloric acid. This allows a better purification of the compound. Aldehyde **6** is then crystallized from a solution in a mixture of tetrahydrofuran and ethyl acetate in the ratio 1:5. The white crystals melt at 160 °C. The ^{1}H-NMR spectrum is consistent with the expected formula.

The procedure followed for the preparation of imine **9** may look a little awkward, yet it turns out to be a comparatively simple way to obtain fairly pure **9**. The first step requires the synthesis of polymer **10**, which has been done following a procedure already described.[7] The formation of the copper complex prevents the –OH group in the ortho position of 2,4-dihydroxybenzaldehyde (which is the key compound) to be involved in the successive ester bond formation. In a typical preparation, ~2 g of polymer **10** are dissolved in 35 mL of warm chloroform. To this solution, cooled to room temperature, are added ~50 mL of water and 2 mL of 37% HCl. After stirring the mixture for a few minutes, the chloroformic phase containing imine **9** is separated, washed with water, and dried. Part of the solvent is then distilled out, and a first crystallization is operated from a 10 mL of chloroform/40 mL of ethanol solution. Further crystallization is obtained utilizing a chloroform/ethanol (1:4 by volume) mixture as a solvent. The ^{1}H-NMR spectrum is consistent with the formula. The compound exhibits polymorphic behavior both in the crystalline and in the mesomorphic state. Melting takes place at 93 °C followed by crystallization to a second crystal form which finally melts at 103 °C with a melting enthalpy of 91 J g^{-1} producing a nematic mesophase. Isotropization takes place at 128 °C with a transition enthalpy of 7.3 J g^{-1}. Supercooling of the nematic phase allows a monotropic second-order phase transition to show up at 92 °C prior to crystallization. At that temperature, an unequivocal textural change is observable in correspondence with a discontinuity of the specific heat detectable by DSC.

Aldehyde **8** was prepared by reaction of 3-methoxy-4-hydroxybenzaldehyde and the appropriate dicarboxylic acid chloride previously prepared according to a procedure already described.[8] In a typical preparation, to 20 mL of an anhydrous chloroform solution of 1.335 g of dicarboxylic acid chloride is added a double amount of 3-methoxy-4-hydroxybenzaldehyde together with ~2 mL of triethylamine. The reaction takes place at room temperature in about 20 min. Dialdehyde **8** is then precipitated by addition of ~80 mL of ethanol. Purification is obtained by crystallization from an ethyl acetate solution. The melting temperature is 137 °C. The ^{1}H NMR spectrum is consistent with the formula.

Network Synthesis. The procedure followed to obtain cross-linked polymers **3**(cl), **4**(cl), and **5**(cl), based respectively on polymers **3**–**5**, is described in detail only for **3**(cl). It applies, mutatis mutandis, to all of them.

A total of 0.541 g (equivalent to 1.049 mmol of –OH groups) of polymer **3** is dissolved under flowing nitrogen in 9.3 mL of anhydrous *o*-dichlorobenzene at 180 °C. The solution is then cooled to 130 °C, and 0.025 16 g (0.0525 mmol) of 4,4′-bis(1,12-dioxydodecane)benzoic acid chloride dissolved in 1 mL of *o*-dichlorobenzene at 130 °C is quickly added under stirring. After ~20 s ~0.82 mmol of tributylamine is added to the solution. Gelation takes place within 15 s. The cross-link reaction is completed in 30 min at 120 °C. This time interval is not sufficient to allow anisotropization of **3**(cl) to occur. Therefore, the swollen network, still in the isotropic state, is then cooled at room temperature, extracted from the reaction vessel, and stored at room temperature in a large volume of *o*-dichlorobenzene for at least 20 days before any examination is undertaken.

The ClOC–/–OH molar ratio utilized in the cross-link reactions is 0.10. This strong excess of –OH groups should make the fraction of completely unreacted dicarboxylic acid chloride molecules quite low. Of course, the cross-link efficiency depends on the amount of molecules actually bridging two different polymer chains. In this respect, molecules linked to the network matrix via a single ester bond are not effective. No measure of this event has been attempted. Therefore, the cross-link density is assumed to be 10% merely as the nominal value.

Model Compounds. Model compound **11** was prepared by reacting equal amounts of aldehyde **12**, previously prepared according to a procedure described elsewhere,[9] and 3-(hexyloxy)-aniline in boiling absolute ethanol for ~3 min. Yellow crystals of **11** are obtained on cooling the solution. Model compound **13** was prepared by reaction of **11** with excess 4-(hexyloxy)benzoic acid chloride at room temperature in a *o*-dichlorobenzene solution in the presence of triethylamine. **13** precipitates at low temperature by addition of ethanol. Further crystallizations were operated from an absolute ethanol solution. Both model compounds have ^{1}H-NMR spectra corresponding to the respective formulas. Their phase behavior will be presented in the Results and Discussion section.

Experimental Methods. The phase behavior was examined by differential scanning calorimetry utilizing a Perkin-Elmer DSC-7 apparatus. Samples were examined under a dry nitrogen flow with a temperature scanning rate of 10 K min^{-1}. Transition temperatures reported in this paper were measured at the

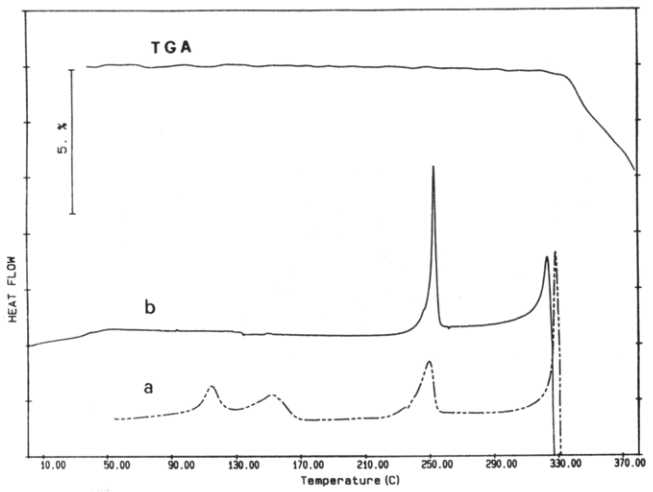

Figure 2. DSC heating curves and thermogravimetric curve for polymer **3**: sample with no previous thermal treatment (a); melt-extruded fiber (b).

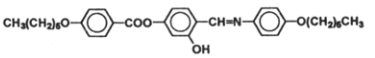

11

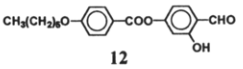

12

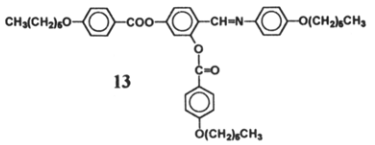

13

maximum of the DSC endotherm. Temperature-controlled polarizing microscopy (Leitz microscope, Linkam microfurnace) was utilized for further analysis of the phase transitions and for the observation of liquid crystalline textures. Samples were examined under a slow dry nitrogen flow. X-ray diffraction patterns were recorded by the flat-film camera photographic method utilizing Ni-filtered Cu Kα radiation. For high-temperature measurements a temperature-controlled microfurnace was used, keeping the samples sealed inside Lindemann capillaries under a nitrogen atmosphere.

In order to obtain better experimental conditions for the study of the liquid crystalline phase, aligned fiber samples were utilized in several cases for the X-ray diffraction analysis. Therefore, the DSC calorimetric behavior of these samples was also examined.

Thermogravimetric (TGA) measurements (Mettler TG50 apparatus) were performed for monitoring the thermal stability of polymers and for measuring the solvent content in swollen cross-linked samples. The viscosity of *o*-dichlorobenzene solutions of linear polymers **3**–**5** was measured at 130 °C utilizing an Ubbelohde viscometer.

Results and Discussion

Linear Polymers. Polymer 3. Figure 2 shows the DSC heating curves for polymer **3** with no previous thermal treatment (curve a) and for fibers extruded from the melt (curve b). The TGA curve is also shown superimposed. The polymer sample used in this analysis and for the preparation of the network has intrinsic viscosity $[\eta]$ = 2.60 dL g^{-1}. Melting of previously untreated samples takes place at ~250 °C, producing an optically anisotropic liquid with enthalpy change ΔH = 19 J g^{-1}. The melting temperature of melt-extruded fibers is not much different, but the transition enthalpy is somewhat larger (~16 J g^{-1}) and both quantities may be brought to higher values by

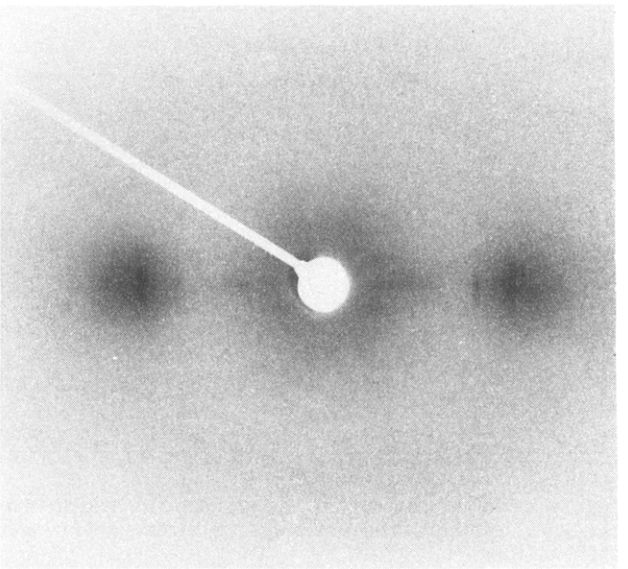

Figure 3. X-ray diffraction pattern for a melt-extruded fiber of polymer **3** recorded at room temperature.

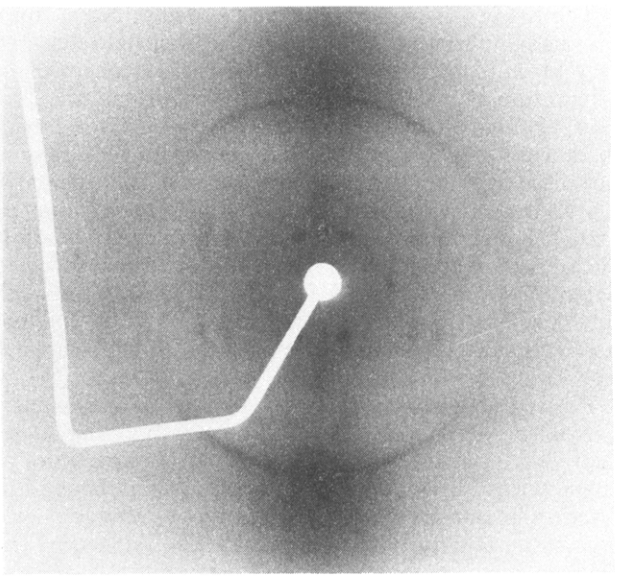

Figure 4. X-ray diffraction pattern recorded at room temperature for a melt-extruded fiber of polymer **3** previously annealed 30 min at 230 °C.

short annealing at ~230 °C (T_m = 268 °C, ΔH = 22 J g^{-1}). Isotropization is hidden by the onset of chemical decomposition. The X-ray diffraction pattern recorded at room temperature for a melt-extruded fiber is reported in Figure 3. It is characterized by two sharp equatorial diffractions (at 4.27 and 5.16 Å lattice distance) and by a weaker, rather diffuse modulation of diffracted intensity outside the equatorial line. The X-ray diffraction pattern recorded at room temperature for a fiber previously annealed 30 min at 230 °C is shown in Figure 4. The pattern is typical for a crystalline, not entirely oriented sample. It is characterized by an equatorial diffraction, at 4.30 Å, of outstanding intensity and by a meridian sharp diffraction at 11.0 Å. The other most intense, nonequatorial Bragg diffractions are found at lattice distances 5.60, 6.19, 7.31, and 14.0 Å. It is not unlikely that the sharpening of the nonequatorial diffractions with respect to the unannealed fibers is more directly related to an improved register of the polymer chain packing along the fiber axis than to an increased degree of crystallinity. However, since the elucidation of the solid-state structure (including the solid-state polymorphism whose occurrence is suggested by the

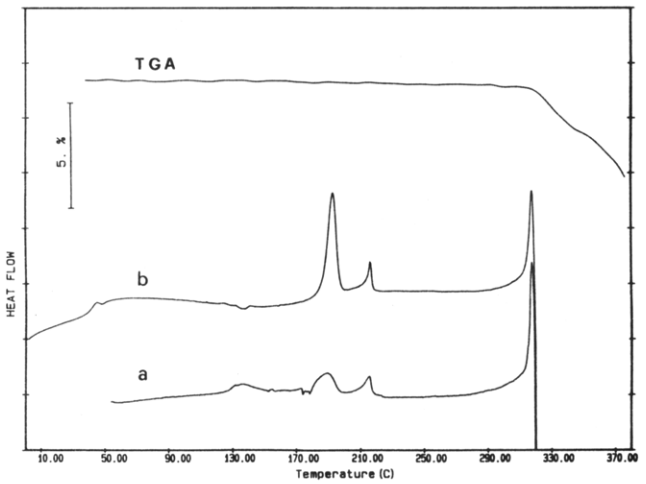

Figure 5. DSC heating curves and thermogravimetric curve for polymer 4: sample with no previous thermal treatment (a); melt-extruded fiber (b).

DSC curve of the untreated sample) is not central to our subject, no further investigation has been carried on.

The X-ray diffraction pattern recorded at 273 °C for a fibrous sample is characterized by a diffuse halo centered around $\sin(\vartheta)/\lambda = 0.1058$ Å^{-1}. The original macroscopic orientation of the polymer chains is lost on melting. No sharp Bragg diffraction has been observed for lattice distances lower than ~38 Å. However, this feature does not necessarily imply that the mesophase must be nematic.

Polymer 4. The phase behavior of polymer 4 is to some extent similar to that described for polymer 3 but exhibits also a relevant peculiarity. The quantitative data reported hereafter were measured for a polymer sample with intrinsic viscosity $[\eta] = 1.52$ dL g^{-1}. The same polymer has been utilized for the preparation of the network discussed later on.

Figure 5 shows the DSC heating curve for a previously untreated sample (curve a). The corresponding X-ray diffraction pattern recorded at room temperature is characterized by a single, slightly broadened Bragg diffraction line at 4.3 Å and is indicative of a very poorly crystalline material. Curve b of Figure 5 concerns the DSC behavior of unannealed melt-extruded fibers. The X-ray diffraction pattern recorded at room temperature is shown in Figure 6. It is characterized by two features: (i) the presence of a sharp and strong Bragg diffraction at 4.5 Å along the equatorial line; (ii) a sharp Bragg diffraction at 21.2 Å accompanied by a diffuse equatorial halo centered around $\sin(\vartheta)/\lambda = 0.104$ Å^{-1}.

The room-temperature X-ray diffraction pattern for a fibrous sample previously brought at 173 °C for a very short time (~1 min) shows only the sharp equatorial diffraction, while the diffraction pattern recorded at 205 °C exhibits the sharp meridian spot and the diffuse equatorial halo (the same diffraction pattern may be obtained by rapid cooling in icy water a fiber extruded from the nematic phase). In both cases the original molecular orientation in the sample is well preserved. A prolonged annealing at 170 °C increases crystallinity both in the fibrous and in the previously untreated polymer which exhibit entirely consistent X-ray diffraction patterns. We might conclude that at room temperature the melt-extruded fiber contains two phases: (1) a mesophase (or a two-dimensional crystalline phase) as for polymer 3 characterized by a close equatorial paking but having a rather defective register of the chains along the fiber axis; (2) a smectic A phase under metastable conditions. In analogy with polymer 3, the endothermic signal at ~190 °C corresponds to the transition from a defective crystal phase (or mesophase) to a proper liquid crystalline phase (smectic A for polymer 4, probably nematic for polymer 3).

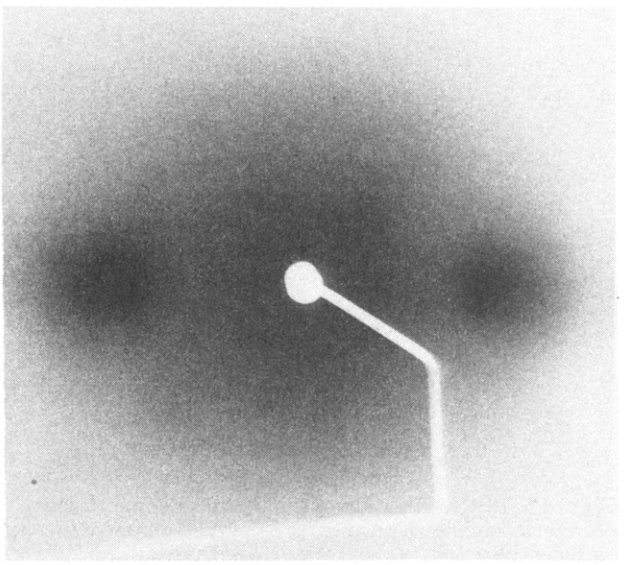

Figure 6. X-ray diffraction pattern recorded at room temperature for a melt-extruded fiber of polymer 4.

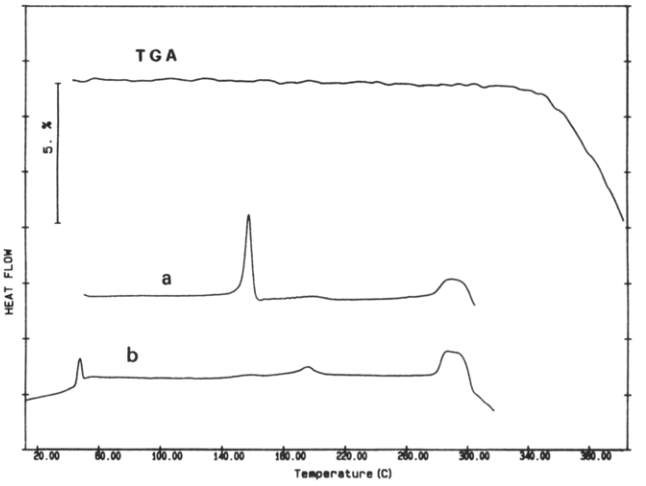

Figure 7. DSC heating curves and thermogravimetric curve for polymer 5: sample with no previous thermal treatment (a); melt-extruded fiber (b).

The endothermic signal shown at 215 °C ($\Delta H = 1.6$ J g^{-1}) in the DSC curves of Figure 5 corresponds to a smectic A–nematic phase transition. This is confirmed by the X-ray diffraction pattern recorded at 225 °C showing only a diffuse halo.

As confirmed by the TGA experiment, isotropization and chemical decomposition overlap to an extent that makes isotropization temperature not measurable.

Polymer 5. The quantitative data reported for this copolymer were measured for a sample having intrinsic viscosity $[\eta] = 1.05$ dL g^{-1}. The same polymer sample was utilized to prepare the cross-linked material whose characteristic features are reported in the next section.

Figure 7 reports the DSC behavior of a previously untreated sample of the polymer (curve a). The corresponding X-ray diffraction pattern recorded at room temperature is indicative of the presence of a crystalline phase. The endothermic signal peaked at 157 °C ($\Delta H =$ 17 J g^{-1}) corresponds to the melting of the crystal phase to an optically anisotropic liquid. No such signal is present in the heating DSC curve obtained from a melt-extruded

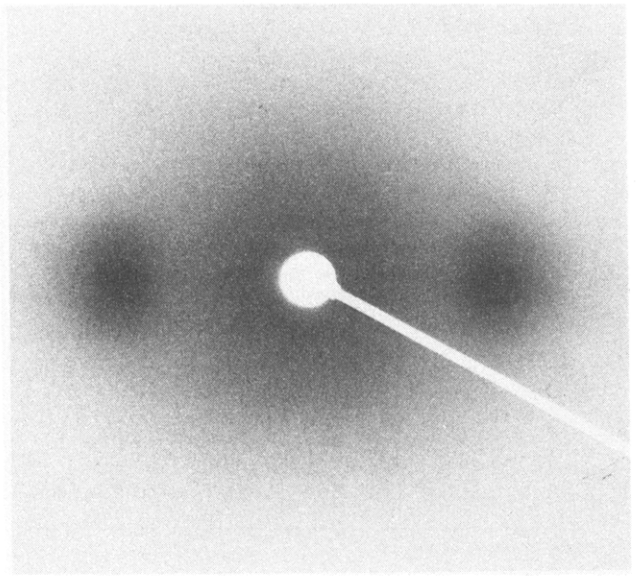

Figure 8. X-ray diffraction pattern recorded at room temperature for a melt-extruded fiber of polymer **5**.

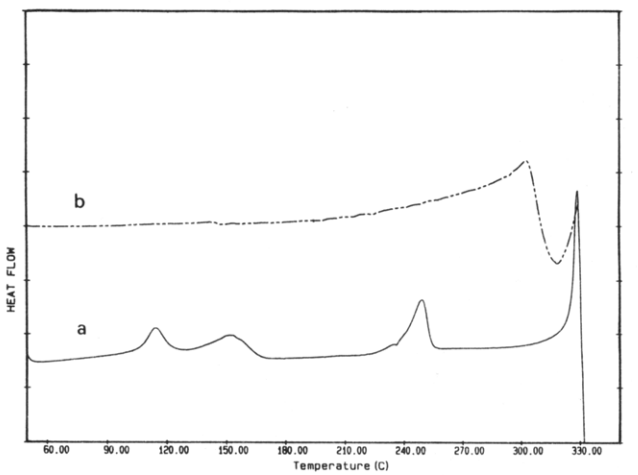

Figure 9. DSC heating curve for network polymer **3**(cl) (curve b) compared to that of a previously untreated sample of linear polymer **3** (curve a).

fiber (curve b of Figure 7). Consistently, the X-ray diffraction pattern recorded at room temperature (Figure 8) shows no evidence of crystalline diffraction and is compatible with a macroscopically oriented liquid crystalline structure such as a nematic or a smectic A or C phase with a smectic periodicity larger than ~29 Å. The broad endotherm at ~290 °C corresponds to the isotropization. A weak endothermic DSC signal is detectable both for untreated and fibrous samples at temperatures (~195 °C) well above melting. Although no consistent textural change was observed by polarizing microscopy, this might be indicative of a liquid phase transition. However, the feature was not investigated any further.

Networks. Networks have been examined after at least 20 days of permanence in a large excess of *o*-dichlorobenzene at room temperature. This allows the virtual completion of the partial deswelling that starts as anisotropization takes place on cooling the freshly cross-linked polymer. Extraction of the solvent from the swollen networks was operated by evaporation in the TGA vessel at 240, 205, and 190 °C respectively for **3**(cl), **4**(cl), and **5**(cl). The solvent loss was continuously monitored until a constant mass was attained. Figure 9 shows the DSC heating curve for a dry sample of **3**(cl) (curve b). Isotropization takes place within a rather broad temperature

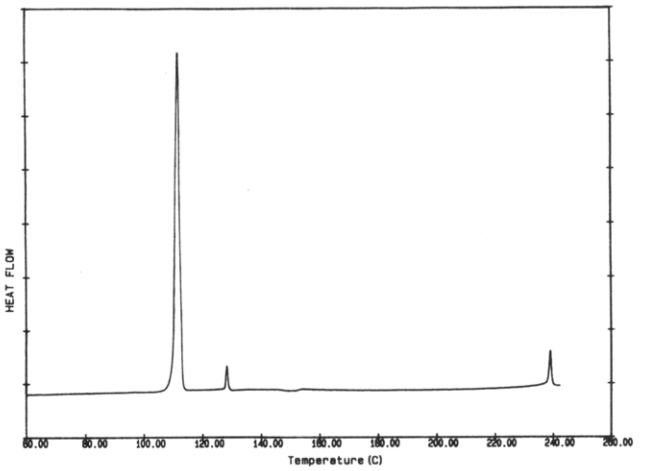

Figure 10. DSC heating curve for model compound **11**.

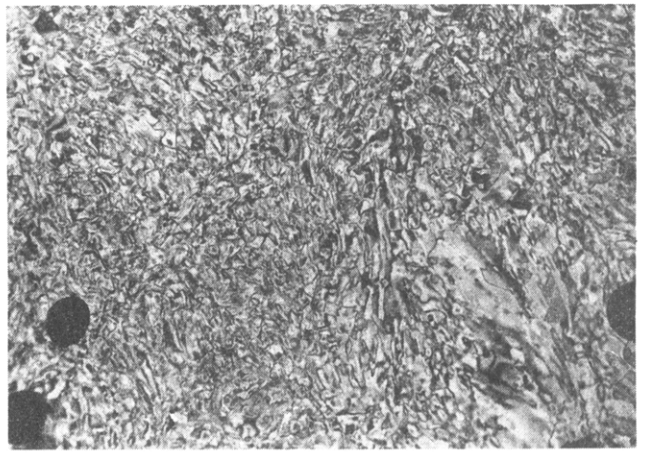

Figure 11. Model compound **11**. Texture of the smectic phase at 112 °C. Crossed polarizers.

interval peaked around ~300 °C and contiguous to the beginning of chemical decomposition. It is apparent, however, that cross-linking depresses the stability of the mesophase with respect to the linear polymer. In fact, isotropization of polymer **3** cannot be observed at temperatures lower than ~330 °C, at which the chemical decomposition becomes relevant (Figures 2 and 9, curves a). This feature has already been observed[2,4,5] and is not unexpected, at least because cross-linking has taken place in the isotropic phase. It is possible, however, that for low cross-link densities, particularly when the cross-linking agent largely affects the shape of the molecular branch point but is still conformationally mobile, a relevant effect is due to the intrinsic decrease of the mesogenic potential of that group rather than being caused mainly by interchain boundaries created by the cross-links. This was shown to be the case for the network based on polymer **2**, and this seems to be the case for network **3**(cl).

Figure 10 shows the heating DSC curve for model compound **11**. Melting occurs at 112 °C (ΔH = 60 J g^{-1}), producing an anisotropic liquid with schlieren morphology (Figure 11). The X-ray diffraction pattern recorded at 120 °C is characterized by a diffuse halo centered around sin (ϑ)/λ = 0.1093 Å^{-1} accompanied by a sharp Bragg diffraction line at 23.8 Å. The mesophase is much likely of smectic C type. The phase transition occurring at 128 °C (ΔH = 1.8 J g^{-1}) leads to a nematic liquid of cybotactic structure. This is confirmed by the schlieren texture (Figure 12) and by the X-ray diffraction pattern recorded at 140 °C. In fact, after the smectic–nematic transition, some spontaneous ordering of the liquid sample takes

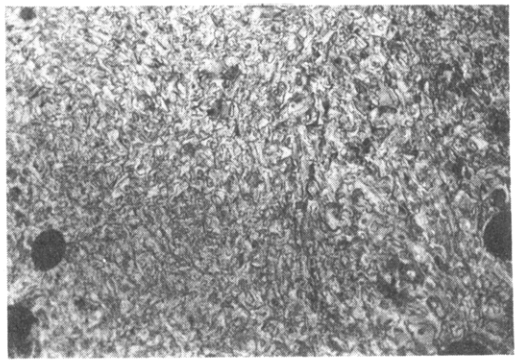

Figure 12. Model compound **11**. Texture of the nematic phase at 161 °C. Same area shown in Figure 11. Crossed polarizers.

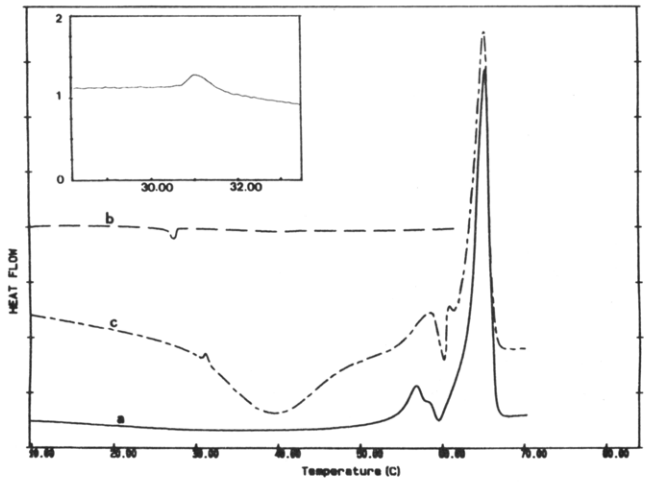

Figure 13. DSC behavior of model compound **13**. Heating curve for a solution-crystallized sample (a); cooling curve (b); second heating curve (c). A section of curve c showing the isotropization is reported on an enlarged scale within the small frame.

place, and besides the equatorial polarization of the diffuse halo, the nonequatorial polarization of a not very sharp but still strong low-angle diffraction is apparent. Finally, isotropization takes place at 239 °C (ΔH = 3.5 J g^{-1}).

The structure of model compound **13** is close to that of a branch group of network **3**(cl). The molecular volume increment with respect to compound **11** is close to 40%. The volume of a branch point in the network should change approximately the same proportion as compared to the original monomer unit. Melting of the solvent-crystallized compounds (Figure 13) occurs at a considerably lower temperature as compared to model **11** (also a solid phase transition does probably occur). The relevant feature is however that an isotropic liquid is formed. A mesophase of probably nematic type is only monotropically formed on cooling (Figure 13, curve b) and may be quenched at room temperature. Since crystallization is slow, mesophase and crystal phases may be easily observed together (Figure 14). Crystallization may be accelerated by heating (Figure 13, curve c), and the isotropization of the noncrystalline fraction (31 °C) is easily detectable both by DSC and by polarizing microscopy. In conclusion, the mesophase stability of model **13** is largely depressed as compared to model **11**. By analogy we might argue that the lower isotropization temperature found for network **3**(cl) with respect to the linear polymer is at least partially caused by an intrinsic loss of mesogenic potential for those polymer segments containing a cross-link as normally observed for binary linear random copolymers containing monomer units of unequal mesogenic attitude.

Figure 15 shows the DSC heating curves of **4**(cl) and

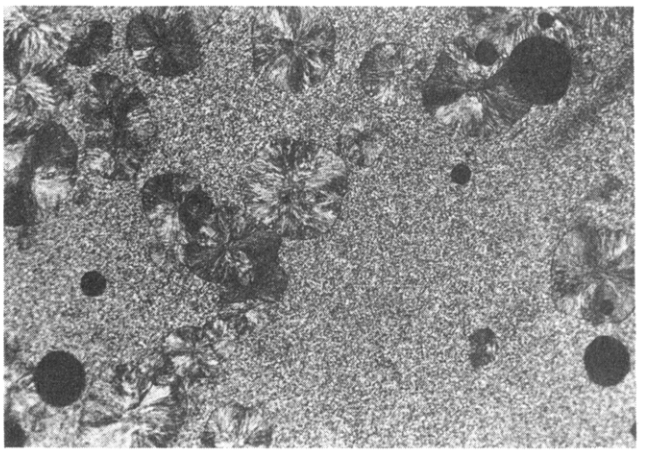

Figure 14. Model compound **13**. Crystallization in progress at 25 °C from the liquid crystalline phase. Crossed polarizers.

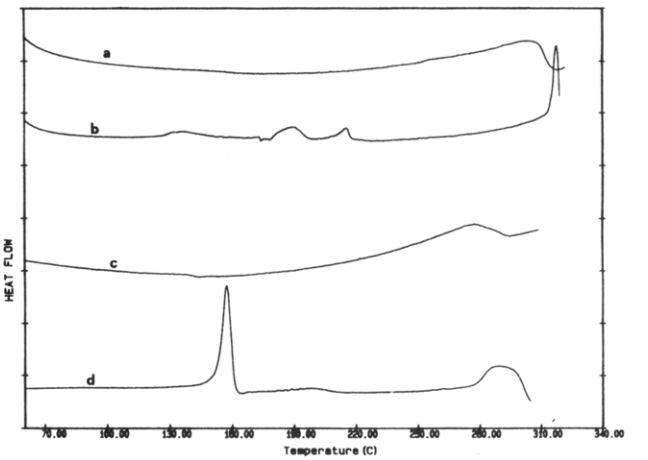

Figure 15. DSC heating curves of networks **4**(cl) (curve a) and **5**(cl) (curve c). The corresponding curves for the linear polymers (curves b and d) are also reported.

5(cl). As for network **3**(cl) isotropization takes place within a broad temperature range with some depression of the mesophase stability. Only for **3**(cl) a faint signal of crystallinity is detectable in the X-ray diffraction pattern recorded at room temperature. For network **5**(cl) the diffraction pattern is characterized by two halos: one is rather strong and is peaked at $\sin(\vartheta)/\lambda = 0.1153$ Å^{-1}; the other is very weak and is peaked at $\sin(\vartheta)/\lambda = 0.0335$ Å^{-1}.

Swollen Networks. The cross-link reaction was performed at 130 °C in an isotropic solution of *o*-dichlorobenzene. A polymer/(polymer + solvent) [$p/(p + s)$] weight ratio ranging between 0.035 and 0.072 was used. The isotropic transparent cross-linked gel undergoes a moderate uniform shrinkage and deswelling as it is cooled to ambient temperature. At the same time, optical anisotropization takes place and the yellow, opaque material takes on a rubbery consistency. For none of the polymers the X-ray diffraction pattern recorded at room temperature contains any sign of crystalline material. Figure 16 shows the DSC behavior for the swollen form of network **3**(cl). Isotropy is recovered by heating the gel and is accompanied by an endothermic effect (Figure 16, curves a and b). Conversely, anisotropization on cooling has an exothermic counterpart also detected by DSC analysis (curve c). Heating and cooling DSC curves for swollen **4**(cl) and **5**(cl) are reported in Figure 17. The first heating curve of **5**(cl) suggests that the transformation into the isotropic phase takes place in two stages. This feature, although in a much less sharp way, is also detectable for **3**(cl).

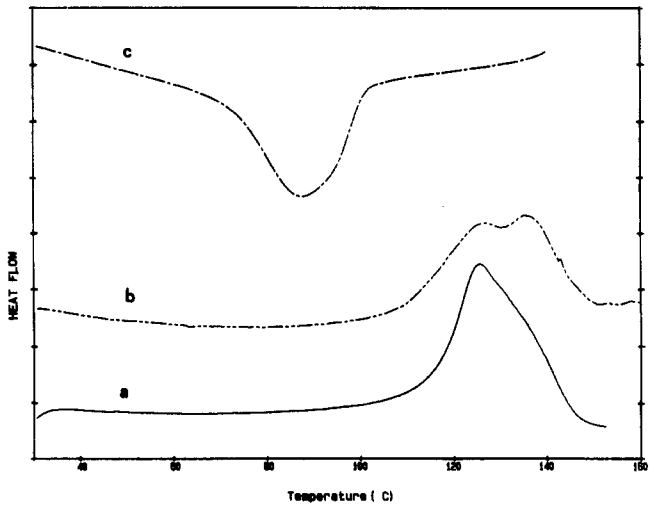

Figure 16. DSC curves for a swollen sample of 3(cl) in the absence of excess solvent: first heating (a); second heating (b); first cooling (c).

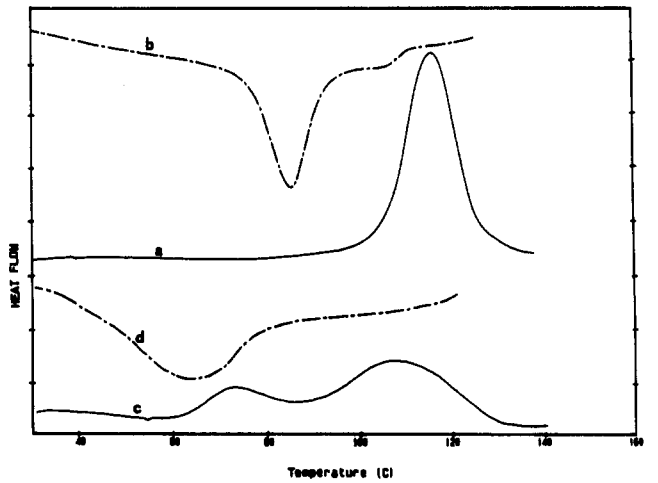

Figure 17. DSC curves for swollen samples of 4(cl) (heating, curve a; cooling, curve b) and 5(cl) (heating, curve c; cooling, curve d) in the absence of excess solvent.

Table 1 reports quantitative data for swollen networks obtained starting with isotropic solutions having two different $p/(p+s)$ weight ratios for each polymer. Higher values for this ratio corresponds to higher values for the correspondent $n/(n+s)$ weight ratio in the anisotropic swollen network at room temperature. In correspondence with that, while isotropization peak temperatures are fairly constant, enthalpic changes are approximately proportional to the polymer content.

Polymers 3–5 possess a considerable conformational flexibility which does not appear to be largely hampered in the corresponding cross-linked networks by interchain constraints. Furthermore, the polymer weight fractions found in the anisotropic swollen state of 3(cl), 4(cl), and 5(cl) are comparable to those characterizing the liquid

Table 1. Isotropization of Swollen Networks: Calorimetric Data[a]

network		$p/(p+s)$	$n/(n+s)$	T_i	ΔH_i
3(cl)	I	0.072	0.106	126	6.7
	II	0.035	0.051	128	3.3
4(cl)	I	0.068	0.127	116	7.0
	II	0.037	0.062	112	4.0
5(cl)	I	0.066	0.129	98	8.0
	II	0.058	0.093	96	5.2

[a] $p/(p+s)$ = polymer/(polymer + solvent) weight fraction in the solution used for cross-linking; $n/(n+s)$ = polymer weight fraction in the anisotropic swollen network at room temperature; T_i/°C = temperature at the maximum of the isotropization DSC endotherm; ΔH_i/(J g^{-1}) = isotropization enthalpy.

crystalline lyotropic solutions of rigid polyaromatics such as poly(1,4-benzamide)[10] or poly(1,4-phenyleneterephthalamide)[11] and considerably smaller than is necessary to obtain anisotropic swollen networks based on cellulose derivatives.[12] On the other hand, the phase behavior of swollen 3(cl), 4(cl), and 5(cl) is similar in its essence to that described for the swollen state of a moderately cross-linked network obtained from polymer 2.[5] A ^{13}C-NMR study of the anisotropic swollen state of this network has shown its multiphase structure characterized by the presence of a major polymer fraction in a noncrystalline solidlike status together with a smaller fraction under isotropic, solutionlike conditions.[13] It is likely that a similar conclusion may apply also to the anisotropic swollen state of 3(cl), 4(cl) and 5(cl). It would also be more consistent with the observed dependence of the apparent degree of swelling, at constant (nominal) cross-link density, on the polymer concentration $p/(p+s)$. A specific ^{13}C-NMR investigation is under way.

Acknowledgment. Research was supported by Consiglio Nazionale delle Ricerche, Progetto Finalizzato Chimica II.

References and Notes

(1) Zentel, R.; Reckert, G. *Makromol. Chem.* **1986**, *187*, 1915.
(2) Bualek, S.; Kapitza, H.; Meyer, J.; Schmidt, G. F.; Zentel, R. *Mol. Cryst., Liq. Cryst.* **1988**, *155*, 47.
(3) Warner, M.; Wang, X. J. *Macromolecules* **1992**, *25*, 445.
(4) Caruso, U.; Centore, R.; Roviello, A.; Sirigu, A. *Macromolecules* **1992**, *25*, 129.
(5) Caruso, U.; Pragliola, S.; Roviello, A.; Sirigu, A. *Macromolecules* **1993**, *26*, 221.
(6) de Gennes, P.-G. *R. Seances Acad. Sci., Ser.* B **1975**, *B281*, 101.
(7) Caruso, U.; Roviello, A.; Sirigu, A. *Macromolecules* **1991**, *24*, 2606.
(8) Griffin, A. C.; Havens, S. J. *J. Polym. Sci., Polym. Phys. Ed.* **1981**, *19*, 951.
(9) Caruso, U.; Roviello, A.; Sirigu, A. *Liq. Cryst.* **1990**, *7*, 421.
(10) Kwolek, S. L.; Morgan, P. W.; Schaefgen, J. R.; Gulrich, L. W. *Macromolecules* **1977**, *10*, 1390.
(11) Bair, T. I.; Morgan, P. W.; Killian, F. L. *Macromolecules* **1977**, *10*, 1396.
(12) Mitchell, G. R.; Guo, W.; Davis, F. J. *Polymer* **1992**, *33*, 68.
(13) Caruso, U.; Perenze, N.; Roviello, A.; Segre, A. L.; Sirigu, A. *Macromol. Rapid Commun.* **1994**, *15*, 357.